

# Interpretation of Soft X-Ray Emission Spectra by Means of Local Solid State Models

Applications to TiC, TiN, TiO, VC, VN and VO

Peter Weinberger

*Institut für Technische Elektrochemie der Technischen Universität Wien,  
Getreidemarkt 9, A-1060 Wien, Austria*

Soft X-ray emission spectra for TiC, TiN, TiO, VC, VN and VO are interpreted in terms of octahedral clusters for these compounds. A comparison of experimental data and theoretically calculated spectra is shown.

**Key words:** X-ray emission spectra, soft ~

## 1. Introduction

At present two different approaches for an interpretation of soft X-ray emission spectra (XES) seem to be commonly used. First, an MO-type description for the electronic structure of the ground state of nearest neighbour clusters [1-6]. Second, an interpretation in terms of local partial density of states functions, as derived from band structure calculations for the ground state crystals [7-9]. Both schemes operate quite successfully within the approximation that the electronic structure for the ground state will be representative of the characteristic sequence of bands (peaks) in the XE spectra.

However, there are only very few attempts to calculate transition probabilities for XE spectra and to compare theoretically convoluted spectra with the corresponding experimental ones.

In the present paper, XE spectra for TiC, TiN, TiO, VC, VN and VO - all compounds crystallizing in the NaCl structure - are interpreted in terms of the ground state for octahedral clusters. The electronic structure for these clusters is calculated by means of the SW-X $\alpha$  method [10-12]. Since a potential field of "muffin-tin" type for a restricted selection of scattering centres will reproduce the crystal potential only moderately well, no attempt is made to calculate the "muffin-tin" charge density for these clusters self-consistently [12].

In order to obtain XE spectra theoretically, transition probabilities are calculated by means of the method summarized in Sect. 2 and broadening effects will be simulated as discussed in Sect. 3.

In Sect. 4, theoretically convoluted XE spectra for the series TiC, TiN, TiO, VC, VN and VO are compared with available experimental data. Finally, in Sect. 5 the applicability of the presented method and the reliability of calculated results will be discussed in terms of the approximations involved.

## 2. Transition Probabilities and Intensities for XE Spectra

In the case of soft X-ray emission, the influx of radiation generates holes in the electronic core states. The emitted radiation is caused by spontaneous transitions of valence electrons to the core holes. Within the theory of dipole emission [13] the intensity of this transition is proportional to the square of the transition moment per unit time,

$$I(\omega) \propto \omega^3 M^2, \quad (1)$$

$\omega$  being the frequency of the radiated quantum. This quantity  $I(\omega)$  can be calculated quite easily within the SW- $X_\alpha$  method, provided that both the initial state as well as the final state can be represented by one-electron orbitals of the ground state (ground state approximation) and that the emitted quantum can be set up in the first place as the difference of the corresponding one-electron eigenvalues, namely for a particular valence state  $\nu$  and core state  $\mu$ ,  $E_\nu$  and  $E_\mu^c$ , respectively:

$$h\omega = E_\nu - E_\mu^c \quad (2)$$

Since core states are completely localized within atomic spheres, a core wave function will be of the form

$$\Psi(\mathbf{z}, E_\mu^c) = \begin{cases} \Phi(\mathbf{z}_p, E_\mu^c); & |\mathbf{z}_p| = |\mathbf{z} - \mathcal{R}_p| < b_p \\ 0, & \text{otherwise,} \end{cases} \quad (3)$$

$\mathcal{R}_p$  being the distance vector from the origin to the centre of the  $p$ th atomic sphere and  $b_p$  the atomic sphere radius.

In the following only the atomic sphere centred in the origin

$$\mathcal{R}_p = 0 \quad 0 \leq |\mathbf{z}| < b \quad (4)$$

shall be considered, since for crystallized compounds the origin of a cluster can always be chosen to be centred in the constituent of most interest, i.e. at the site where the transition occurs.

As one can see from (3), any scalar product of the type

$$\langle \Psi(\mathbf{z}, E_\mu^c) | \Psi(\mathbf{z}, E_\nu) \rangle \quad (5)$$

has to be calculated solely within atomic spheres. According to (4), only the sphere centred in the origin of the cluster has to be considered.

Within a region of spherical symmetric potential, the wave function  $\Psi(\mathbf{z}, E_\nu)$  to the valence eigenvalue  $E_\nu$  is expanded into partial waves

$$\Psi(\mathbf{z}, E_\nu) = \sum_{lm} c_{lm}^\nu u_l(r, E_\nu) Y_{lm}(\hat{\mathbf{z}}). \quad (6)$$

In (6)  $u_l(r, E_\nu)$  is the solution of the radial Schrödinger equation for the eigenvalue  $E_\nu$  and angular momentum  $l$  and  $c_{lm}^\nu$  the eigenvector (see Eq. (2.18) of Ref. [12]).

In the case of a core state  $E_\mu^c$ , it is sufficient to consider only one partial wave

$$\Psi(\mathbf{z}, E_\mu^c) = c_{lm}^\mu u_l(r, E_\mu^c) Y_{lm}(\hat{\mathbf{z}}). \quad (7)$$

Choosing the coefficient  $c_{lm}^\mu$  to be unity implies the following normalization for the core wave function:

$$\Psi(z, E_\mu^c) = [R_l^\mu]^{-1} u_l(r, E_\mu^c) Y_{lm}(\hat{z}), \quad (8)$$

where  $R_l^\mu$  is given by

$$R_l^\mu = \int_0^b u_l^2(r, E_\mu^c) r^2 dr. \quad (9)$$

The components of the electric  $2^l$ -pole momentum operator can be set up in terms of harmonic polynomials,

$$\mathcal{Y}_{lm}(z) = r^l Y_{lm}(\hat{z}), \quad (10)$$

where  $l = 1$  in the case of the dipole approximation.

According to (6, 8, 10), a particular component of the transition moment will be given by

$$\begin{aligned} M_{l_1 m_1, l_2 m_2}^{\mu\nu} &= [R_{l_1}^\mu]^{-1} \sum_{l_3 m_3} c_{l_3 m_3}^\nu \langle u_{l_1}(r, E_\mu^c) Y_{l_1 m_1}(\hat{z}) | r^{l_2} Y_{l_2 m_2}(\hat{z}) \\ &\quad | u_{l_3}(r, E_\nu) Y_{l_3 m_3}(\hat{z}) \rangle = \\ &= [R_{l_1}^\mu]^{-1} \sum_{l_3 m_3} c_{l_3 m_3}^\nu R_{l_1 l_2 l_3}^{\mu\nu} \left[ \frac{(2l_1 + 1)(2l_2 + 1)(2l_3 + 1)}{4\pi} \right]^{1/2} \times \\ &\quad \times \begin{pmatrix} l_1 & l_2 & l_3 \\ 0 & 0 & 0 \end{pmatrix} \begin{pmatrix} l_1 & l_2 & l_3 \\ m_1 & m_2 & m_3 \end{pmatrix}. \end{aligned} \quad (11)$$

In (11)  $R_{l_1 l_2 l_3}^{\mu\nu}$  is the radial part of the integration

$$R_{l_1 l_2 l_3}^{\mu\nu} = \int_0^b u_{l_1}(r, E_\mu^c) r^{l_2 + 2} u_{l_3}(r, E_\nu) dr. \quad (12)$$

The angular part of the integral can be expressed in terms of Clebsch-Gordon coefficients, which automatically provide selection rules, since

$$|l_1 - l_3| < l_2 < l_1 + l_3. \quad (13)$$

The transition probability corresponding to (11) will then be

$$\begin{aligned} |M_{l_1 m_1, l_2 m_2}^{\mu\nu}|^2 &= [R_{l_1}^\mu]^{-2} \left[ \frac{(2l_1 + 1)(2l_2 + 1)}{4\pi} \right] \sum_{l_3 m_3} \sum_{l_3' m_3'} c_{l_3 m_3}^\nu c_{l_3' m_3'}^\nu \times \\ &\quad \times R_{l_1 l_2 l_3}^{\mu\nu} R_{l_1 l_2 l_3'}^{\mu\nu} [(2l_3 + 1)(2l_3' + 1)]^{1/2} \begin{pmatrix} l_1 & l_2 & l_3 \\ 0 & 0 & 0 \end{pmatrix} \begin{pmatrix} l_1 & l_2 & l_3' \\ 0 & 0 & 0 \end{pmatrix} \\ &\quad \times \begin{pmatrix} l_1 & l_2 & l_3 \\ m_1 & m_2 & m_3 \end{pmatrix} \begin{pmatrix} l_1 & l_2 & l_3' \\ m_1 & m_2 & m_3' \end{pmatrix}. \end{aligned} \quad (14)$$

In order to get the total transition probability, one has to sum over all components ( $m_2$ ) of the electric  $2^l$ -pole and over all degenerate core states ( $m_1$ ). Utilizing the orthogonality of Clebsch-Gordon coefficients [14]

$$\sum_{m_1, m_2} \begin{pmatrix} l_1 & l_2 & l_3 \\ m_1 & m_2 & m_3 \end{pmatrix} \begin{pmatrix} l_1 & l_2 & l'_3 \\ m_1 & m_2 & m'_3 \end{pmatrix} = (2l_3 + 1)^{-1} \delta_{l_3 l'_3} \delta_{m_3 m'_3} \quad (15)$$

the total transition probability is

$$\begin{aligned} |M_{l_1, l_2}^{\mu\nu}|^2 &= \sum_{m_1, m_2} |M_{l_1 m_1, l_2 m_2}^{\mu\nu}|^2 = [R_{l_1}^{\mu}]^{-2} \left[ \frac{(2l_1 + 1)(2l_2 + 1)}{4\pi} \right] \times \\ &\times \sum_{l_3} [R_{l_1 l_2 l_3}^{\mu\nu}]^2 \begin{pmatrix} l_1 & l_2 & l_3 \\ 0 & 0 & 0 \end{pmatrix}^3 \sum_{m_3} |c_{l_3 m_3}^{\nu}|^2. \end{aligned} \quad (16)$$

Finally the last sum in (16) can be set up in terms of an  $l$ -like charge  $Q_l^{\nu}$  and an integral of the type as defined in (9)

$$\sum_{m_3} |c_{l_3 m_3}^{\nu}|^2 = Q_{l_3}^{\nu} [R_{l_3}^{\nu}]^{-1}. \quad (17)$$

Within the dipole approximation, the intensity for an XE transition from a valence state  $E_{\nu}$  to a particular core state  $E_{\mu}^c$ , characterized by the angular momentum  $l$ , will therefore be simply given by

$$I^{\mu\nu}(E) \propto E^3 [R_l^{\mu}]^{-2} \frac{3(2l+1)}{4\pi} \sum_{l'} \begin{pmatrix} l & 1 & l \\ 0 & 0 & 0 \end{pmatrix}^2 [R_{l'}^{\nu}]^{-1} R_{ll'}^{\mu\nu} Q_{l'}^{\nu}. \quad (18)$$

The Clebsch-Gordon coefficients which appear in (16) and (18) are easily obtained by means of the following formula [14]

$$\begin{pmatrix} l_1 & l_2 & l_3 \\ 0 & 0 & 0 \end{pmatrix} = \begin{cases} 0; & l_1 + l_2 + l_3 = 2p + 1; \quad p \text{ integer number} \\ (-1)^p \left[ \frac{(l_1 + l_2 - l_3)!(l_2 + l_3 - l_1)!(l_3 + l_1 - l_2)!}{(l_1 + l_2 + l_3 + 1)!} \right]^{1/2} \\ \cdot \frac{p!}{(p - l_1)!(p - l_2)!(p - l_3)!}; & l_1 + l_2 + l_3 = 2p. \end{cases} \quad (19)$$

### 3. Broadening Effects and Convolution of Spectra

Within the approximations mentioned, the intensity for a particular transition  $\mu \rightarrow \nu$  can be calculated by means of (18). However, there is a variety of effects which cause broadening of lines and which cannot be included directly into a simple one-electron theory. It is therefore necessary to correct the calculated intensity parametrically at least with respect to life-time broadening for the core states as well as for valence states and with respect to the spectrometer resolution.

In the present paper the following broadening function of Lorentzian type is used [9, 15]

$$I_1^{\mu\nu}(E) = \pi^{-1} I_0^{\mu\nu}(E_l) \frac{\gamma(E)|2}{(E - E_l)^2 + \gamma(E)^2|4} \quad (20)$$

where  $I_0^{\mu\nu}(E_i)$  is the intensity as defined in (18) and the energy-dependent half-width,  $\gamma(E)$ , can be approximated [15] by

$$\gamma(E) = \gamma_0 + W \left( 1 - \frac{E - E_0}{E_F - E_0} \right)^2 \quad (21)$$

$\gamma_0$  will take care of the life-time broadening for core states and the second term [15] corrects with respect to the valence state broadening. In (21)  $E_0$  is the lowest valence state and  $E_F$  the Fermi energy.

The total life-time corrected intensity will then be a superposition (22) of intensities  $I_1^{\mu\nu}(E)$  (20),

$$I_1^{\mu}(E) = \sum_{\nu} I_1^{\mu\nu}(E), \quad (22)$$

which has to be folded with the spectrometer function

$$I_2^{\mu}(E) = \int_{-\infty}^{\infty} I_1^{\mu}(E') f(E - E') dE'.$$

The spectrometer function will again be of Lorentzian type with a suitable half-width parameter  $S$ .

As can be seen in (21), direct application of this formula requires the explicit knowledge of the Fermi energy  $E_F$ , a quantity which will not be available in terms of a simple cluster calculation. However, since XE spectra are usually presented in a relative energy scale,  $E_F$  corresponding to zero energy, the energy scale of the calculated spectrum can be shifted to a particular peak in the experimental spectrum.

In the present paper all theoretical XE spectra for one compound are convoluted with respect to the corresponding  $K_{\beta_s}^{\text{II}}$  peak in the experimental metal  $K$  spectrum.

#### 4. Applications to TiC, TiN, TiO, VC, VN and VO

Two types of octahedral clusters are investigated, namely  $\text{MeX}_6$  and  $\text{Me}_6\text{X}$  (Me = metal, X = non-metal). Both types are calculated with respect to the same constant potential in the interatomic region [12]. Exchange parameters and atomic sphere radii are chosen according to the values used by Neckel *et al.* [16].

Since the components of the dipole moment operator are transformed according to a particular irreducible representation of the invariance group of the unperturbed Hamilton operator, application of group theory proves to be quite useful for the convolution of theoretical spectra and for an interpretation of the experimental data. For the central sphere, in case of the  $O_h$  point group, only transitions from  $t_{1u}$  valence states for  $K$  spectra and transitions from  $a_{1g}$ ,  $e_g$  and  $t_{2g}$  valence states in case of  $L$  spectra have to be considered.

Since the usual concept of the Fermi energy cannot be applied, the question of the highest occupied state and its occupation number is rather a delicate problem. In the case of nitrides and oxides, where "p"- and "d"-like valence states are separated, these states can be occupied similar to the electronic configuration of the diatomic compounds  $\text{MeX}$ . Thus, in case of clusters of the type  $\text{MeX}_6$ , one ought to consider complex anions such as  $[\text{MeN}_6]^{15-}$  and  $[\text{MeO}_6]^{10-}$ . For these clusters the highest occupied state will be  $2t_{2g}$  and its occupation number refers to the occupation number of the  $3\sigma(2\pi)$  state in the corresponding diatomic molecule  $\text{MeX}$ .

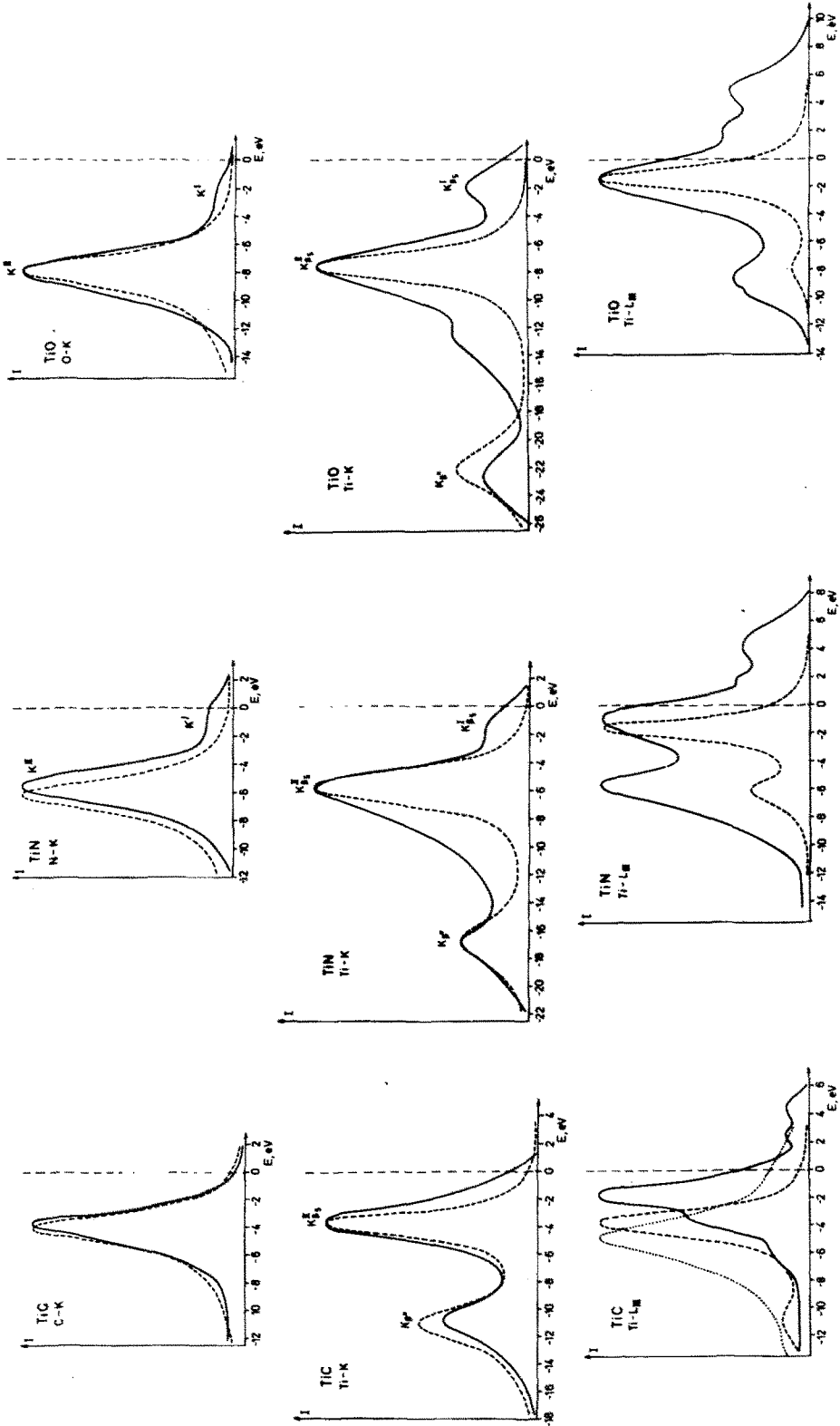


Fig. 1. XE spectra for TIC, TIN and TiO. The top row corresponds to the non-metal K spectrum, the middle row to the metal K spectrum and the lower row to the metal L<sub>II,III</sub> spectrum. Experimental data are shown as full (dotted) lines and theoretical spectra as broken lines. For Refs. see Table 1

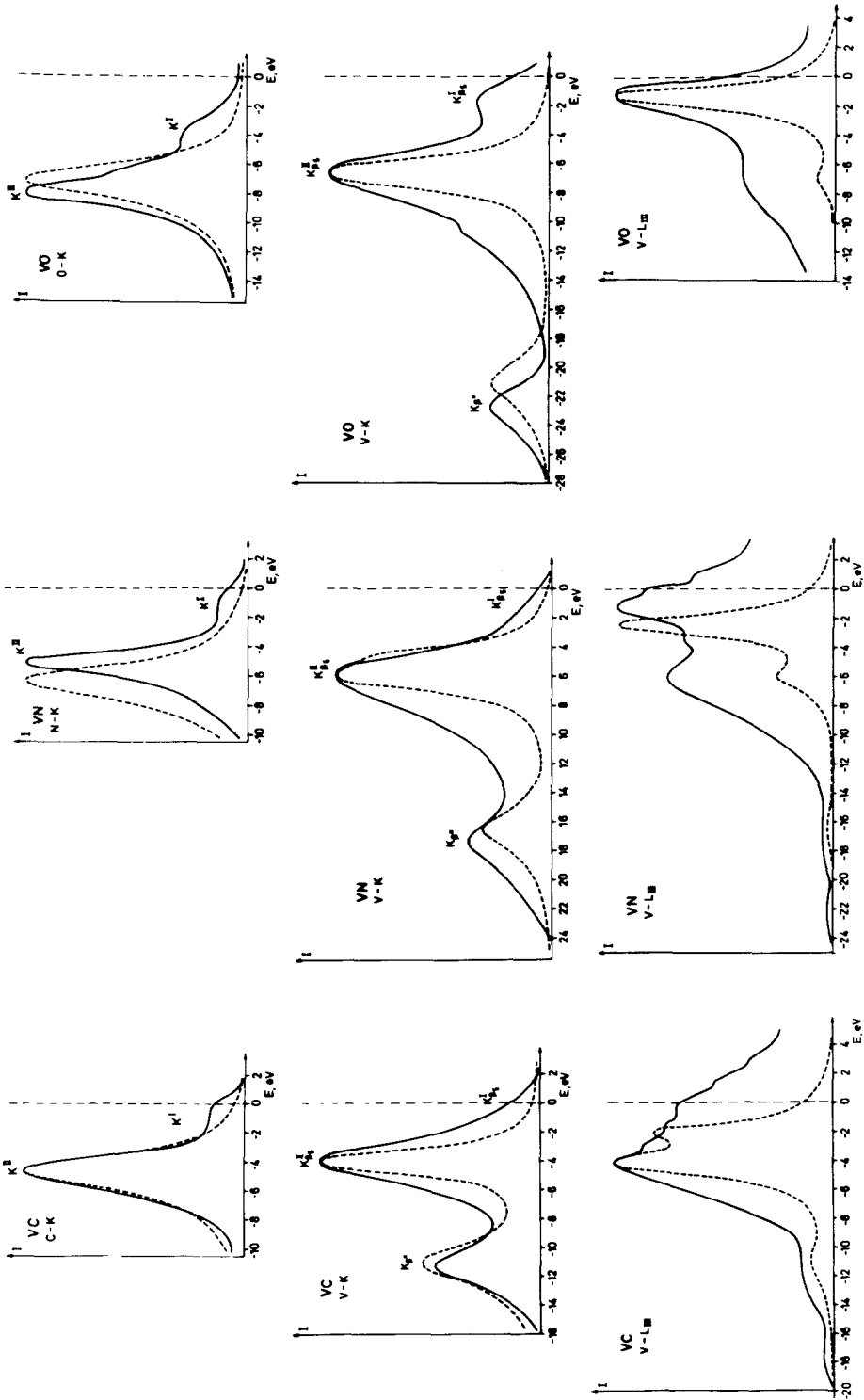


Fig. 2. XE spectra for VC, VN and VO. The top row corresponds to the non-metal K spectrum, the middle row to the metal K spectrum and the lower row to the metal L<sub>II, III</sub> spectrum. Experimental data are shown as full lines and theoretical spectra as broken lines. For Refs. see Table 1

Table 1. References to experimental XE spectra for TiC, TiN, TiO, VC, VN and VO

Compound	Metal <i>K</i>	Metal <i>L</i>	Non-metal <i>K</i>
TiC	<u>17</u> , <sup>a</sup> 18, 23	<u>20</u> , <u>21</u> , <sup>b</sup> <u>22</u> , <sup>b</sup> 24, 27	<u>21</u> , 24, 27, 31
TiN	<u>17</u> , 18, 23	1, <u>20</u> , 25	25, <u>31</u> , 32
TiO	1, <u>17</u> , 18, 23	1, <u>20</u> , 25, 26, 29, 33	20, <u>31</u> , 33
VC	<u>19</u> , 28	1, 25, 28, <u>30</u>	<u>21</u> , 27, 28
VN	<u>19</u>	1, 25, <u>30</u>	<u>24</u> , 32
VO	<u>19</u>	<u>25</u> , 33	<u>24</u> , 33

<sup>a</sup> Underlined Refs. refer to those spectra used in Figs. 1 and 2.

<sup>b</sup> Refer to the dotted line in Fig. 1.

For carbides, there is no such clear-cut situation for “*p*”- and “*d*”-like states. Since in the case of VC<sub>6</sub> the  $2t_{2g}$  state is below the  $3t_{1u}$  state, occupation of the  $3t_{1u}$  state would imply unpaired electrons, localized mainly on the non-metal ligands. This seems to be rather unrealistic [6]. The  $2t_{2g}$  state is therefore assumed to be the highest occupied state with an occupation number corresponding to the top valence orbital in the diatomic molecule VC. According to these considerations, occupation of valence states, corresponding to complex anions of the type [MeC<sub>6</sub>]<sup>14-</sup>, is assumed for the metal XE spectra in TiC and VC.

The comparison of theoretical and experimental spectra is shown for the titanium series in Fig. 1 and for the vanadium compounds in Fig. 2. In both figures, the top row corresponds to the non-metal *K* spectrum, the middle row to the metal *K* spectrum and the lower row to the metal *L* spectrum. The experimental data refer to the  $L_{II,III}$  spectra, the calculated ones to the  $L_{III}$  spectra. Experimental data are shown as full lines and theoretical spectra as broken lines. In case of the Ti  $L_{II,III}$  spectrum in TiC a second experimental spectrum is plotted (dotted line). In Table 1 the references are listed in which the experimental spectra have been published. In this table, underlined references refer to the spectra shown in Fig. 1 and 2. All theoretical metal spectra are calculated with  $\gamma_0 = 0.7$  eV,  $W = 2.0$  eV and  $S = 1.0$  eV, whereas the non-metal *K* spectra are based on  $\gamma_0 = W = S = 1.0$  eV. In all cases  $E_0(21)$  is the corresponding lowest  $a_{1g}$  valence state.

In the following the various types of XE spectra shall be discussed separately.

#### 4.1. Metal *K* Spectra

Figs. 1 and 2 show that for metal *K* spectra the  $K_{\beta_s}^I$  cannot be interpreted in terms of transitions to the central atom in octahedral clusters [MeX<sub>6</sub>]<sup>*n*-</sup>. Comparing corresponding metal *K* and *L* spectra, it is evident that the  $K_{\beta_s}^I$  peak has to be associated with transitions from valence states with predominantly “*d*” character.

In the literature [1, 6], the  $K_{\beta_s}^I$  peak is frequently interpreted in terms of clusters [Me<sub>6</sub>X]<sup>*m*</sup>, namely in terms of transitions from  $a_{1g}$ ,  $e_g$ ,  $t_{1u}$ ,  $t_{1g}$ ,  $t_{2u}$  and  $t_{2g}$  ligand orbitals – corresponding to the splitting of the atomic *d* orbital of the metal – to the proper ligand core orbitals ( $a_{1g}$ ,  $e_g$ ,  $t_{1u}$ ). In this case, the calculation of the transition probabilities cannot be restricted to one sphere (4).

However, it seems to be more appropriate to consider clusters including second neighbour interactions (metal–metal interactions). Expanding the wave function in the central sphere



(6) for orbitals derived from the atomic  $d$  states of the second neighbours will then allow a calculation of the intensity for  $K\beta_5^I$  peaks in terms of the method presented in Sect. 2. In this case only  $t_{1u}$  valence orbitals contribute to the metal  $K$  spectrum.

Irrespective of whether one considers first or second neighbour clusters, in the case of metal  $K$  spectra the  $p$ -like charge within the central metal sphere (17) will always be a small component in the distribution of charges (24) for any  $t_{1u}$  orbital,

$$n_\nu = Q_{\text{in}}^\nu + Q_{\text{out}}^\nu + \sum_{p=1}^N \sum_l Q_{pl}^\nu. \quad (24)$$

In (24)  $n_\nu$  is the degeneracy for the state  $\nu$ ,  $Q_{\text{in}}^\nu$  the charge within the interatomic region,  $Q_{\text{out}}^\nu$  the charge outside the outer sphere,  $N$  the total number of atomic centres in the cluster and  $Q_{pl}^\nu$  the  $l$ -like charge in sphere  $p$  (for reference see Sect. 4 of Ref. [12]).

#### 4.2. Non-Metal $K$ Spectra

Similar to the  $K\beta_5^I$  peak in the metal  $K$  spectrum, the  $K I$  band corresponds to transitions from valence orbitals with predominantly metal “ $d$ ”-character.

However, for clusters of the type  $\text{Me}_6\text{X}$ , on which the analysis for the non-metal  $K$  spectra is based, the  $p$ -like charge in the central non-metal sphere (17) is the dominant component in the distribution of charges (24) for the  $1t_{1u}$  valence state, which corresponds to the atomic  $2p$  levels of the non-metal.

All other  $t_{1u}$  valence states are due to the splitting of the atomic  $d$ -orbitals of the metal ligands. The  $p$ -like charge for these  $t_{1u}$  valence orbitals in the non-metal sphere will add only very little in the resolution of charges. The transition probability from the  $2t_{1u}$  valence orbital to the non-metal core orbital is therefore very much smaller than from the  $1t_{1u}$  orbital. This is the reason why the  $K I$  band in the non-metal  $K$  spectra cannot be resolved properly within a simple first neighbour cluster model. Including a second shell of ligands in case of the non-metal  $K$  spectra will definitely give some information about the asymmetry of the  $K II$  band, but does not seem to be sufficient to improve the theoretical intensity for the  $K I$  peak considerably. In order to interpret this peak properly, results of band structure calculations [8, 9, 16] have to be considered.

#### 4.3. Metal $L$ Spectra

Since the experimental metal  $L$  spectrum is a superposition of the  $L_{II}$  and  $L_{III}$  spectra where corresponding peaks are separated approximately by the atomic spin-orbit splitting parameter (Ti: 5.77 eV, V: 7.10 eV [34]), the theoretical  $L_{III}$  spectrum as calculated for a cluster  $\text{MeX}_6$  can be used in terms of a qualitative interpretation of the experimental data. Taking a typical example, the Ti  $L_{III}$  spectrum in TiO (Fig. 1), one can see that in the theoretical  $L_{III}$  spectrum the main peak, which is due to a transition from the  $2t_{2g}$  valence state to the “ $2p$ ” core state in titanium, is obviously overestimated. This can be explained in the following way. Since the  $2t_{2g}$  state should be occupied only with an integer number of electrons, the transition probability for the main peak and, therefore, the ratio of intensities for the first and second peak in the theoretical spectrum, suffer from this restriction. This is connected with the fact that it is only the  $2t_{2g}$  state which characterizes the occupied part of the “ $d$ ” band in the solid. Considering therefore a cluster with an additional shell of metal ligands will not only improve the width of the main peak in the  $L_{III}$  spectrum, but also the ratio of intensities.

A special case is the  $L_{III}$  spectrum in VC. Because the  $\pi$ -binding character of the  $1t_{2g}$  orbital is decreased substantially going from VO to VN and VC, transitions from the  $1t_{2g}$  as well as from the  $2t_{2g}$  valence state have comparative probabilities. Thus the experimental V  $L_{II,III}$  spectrum in VC can be interpreted quite satisfactorily [9].

## 5. Discussion

In general, considering first neighbour clusters only, the position of the calculated bands is in reasonably good agreement with the experimental data. For metal  $K$  spectra, the energy difference between the  $K_{\beta}''$  and  $K_{\beta_s}''$  peaks can be reproduced within an error bound of 2 eV. This is about the result which one can expect from self-consistent bandstructure calculation [8, 9, 16]. The calculated intensity, based on the "ground state approximation" and the dipole approximation, resolves the experimental metal  $K$  spectra sufficiently well. In the case of the metal  $L$  spectra, the position of bands is reproduced within an error bound of about 1.5 eV.

There is a series of disadvantages which have to be taken into account when considering first neighbour clusters only. First, the  $K_{\beta_s}''$  band in the metal  $K$  spectra cannot be resolved in terms of the method proposed. Second, the ratio of the calculated intensities for metal  $L$  spectra suffers severely from the restriction to first neighbour clusters. Third, the intensity for the  $KI$  band in the non-metal  $K$  spectra is resolved only very badly.

The main disadvantage, however, is that in a simple cluster approach the Fermi energy cannot be calculated directly as in the case of band structure calculations. One has to make assumptions about the ionicity of the clusters.

For the final shape of the theoretical spectra the choice of the parameters  $\gamma_0$ ,  $W$  and  $S$  (21, 23) is obviously of some importance. As one can see in (21), application of an energy-dependent half-width parameter  $\gamma(E)$  will simulate the corresponding asymmetry in the experimental peaks. However, since this effect is of minor importance,  $\gamma(E)$  can also be approximated by a sufficiently large constant ( $\sim 2$  eV). Because there is only a small number of states which contribute to a particular peak, the choice of the parameter  $S$  will be rather important. The crucial test in the case of the clusters  $\text{MeX}_6$  is the  $K_{\beta_s}''$  peak in the metal  $K$  spectra, where transitions from the  $2t_{1u}$  and  $3t_{1u}$  valence state can contribute. Choosing the parameter  $S$  too small can cause an "artificial" split in the theoretical  $K_{\beta_s}''$  peak.

Since relaxation effects can be assumed to be very large indeed, (2) should not be used to predict the absolute position of XE spectra. In the case of the metal  $K$  spectrum [18] in TiC the maximum of the  $K_{\beta}''$  and the  $K_{\beta_s}''$  peak is at 4954 eV and 4961 eV, respectively, while an application of (2) would predict these two peaks to be at 4818.85 eV and 4826.12 eV. Application of the transition state concept [10, 12] gives 4967.6 and 4974.8 eV, which is in reasonably good agreement with the experimental data. However, in the context of XE spectra the transition state concept has two major disadvantages. First, a proper calculation of transition energies requires self-consistency, which will be based on somewhat different models in the case of the SW-X $\alpha$  method [12] and in the case of band structure calculations [35]. Second, though the transition state concept can be a useful tool to approximate transition energies, i.e. the difference of the total energy for two states, the wave functions corresponding formally to the one-electron states of the transition state [36] have never been analysed in terms of scalar products such as (1) and

subsequently (18). Therefore no experience at all is available about the physical meaning of those states.

Relaxing a metal core state will affect essentially orbitals located mainly at the metal constituent, while typical ligand orbitals will be relaxed only very little. Applying therefore one-electron wave functions of the transition state to (18) may be quite misleading.

It was the aim of the present paper to show that simple local models can be applied quite successfully to typical solid state problems [37]. Considering the small computational effort involved, the method presented seems to be applicable for a variety of chemically interesting systems, especially to those where band structure calculations are too tedious or, at present, not possible. It should be noted, however, that results based on a nearest neighbour cluster approach for the solid state will always be only an approximation to those reflecting the full periodicity of the crystal potential.

*Acknowledgement.* The author is grateful to Prof. A. Neckel and Dr. K. Schwarz for many discussions. The computations were performed using the facilities of the Technical University of Vienna Computing Centre.

## References

1. Fischer, D. W.: *J. Appl. Phys.* **41**, 3561 (1970)
2. Fischer, D. W., in: *Bandstructure spectroscopy of metals and alloys*, Fabian, D. J., Watson, L. M., Eds., p. 669. London-New York: Academic Press 1973
3. Tossell, J. A., Vaughan, D. J., Johnson, K. H.: *Nature Phys. Sci.* **244**, 42 (1973)
4. Tossell, J. A., Vaughan, D. J., Johnson, K. H., *Chem. Phys. Letters* **20**, 329 (1973); Tossell, J. A., Vaughan, D. J., Johnson, K. H.: *Am. Mineral.* **59**, 319 (1974); Tossell, J. A.: *J. Electron. Spectr.* **8**, 1 (1976)
5. Slater, R. A., Urch, D. S., in: *Bandstructure spectroscopy of metals and alloys*, Fabian, D. J., Watson, L. M., Eds., p. 655. London-New York: Academic Press 1973
6. Gubanov, V. A., Kasimov, B. G., Kurmaev, E. Z.: *J. Phys. Chem. Solids* **36**, 861 (1975)
7. Conklin, J. B. Jr., Averill, F. W., Hattox, T. M.: *J. Physique* **33**, 213 (1972)
8. Neckel, A., Schwarz, K., Eibler, R., Rastl, P., Weinberger, P.: *Microchim. Acta Suppl.* **6**, 257 (1975)
9. Schwarz, K., Neckel, A.: *Ber. Bunsenges. physik. Chem.* **79**, 1053 (1975)
10. Slater, J. C.: *Advan. Quantum Chem.* **6**, 1 (1972)
11. Johnson, K. H.: *Advan. Quantum Chem.* **7**, 143 (1973)
12. Weinberger, P., Schwarz, K., in: *Intern. Rev. Sci., Phys. Chem. Ser. II, Vol. 1*, p. 255, Buckingham, A. D., Coulson, C. A., Eds. London: Butterworths 1975
13. Kompanyets, A. S.: *Theoretical Physics*, p. 362. Moscow: Foreign Language Publishing House 1961; Messiah, A.: *Quantum mechanics, Vol. II*, p. 1041. Amsterdam: North Holland Publ. Comp. 1969
14. Messiah, A.: *Quantum mechanics, Vol. II, App. C*, p. 1053. Amsterdam: North Holland Publ. Comp. 1969
15. Blokhin, M. A., Sachenko, V. P.: *Izv. Akad. Nauk SSR ser. fiz.* **24**, 397 (1960)
16. Neckel, A., Rastl, P., Eibler, R., Weinberger, P., Schwarz, K.: *J. Phys. C. Solid State Phys.* **9**, 579 (1976)
17. Nemnonov, S. A., Kolobova, K. M.: *Fiz. metal metalloved* **22**, 680 (1966)
18. Ramqvist, L., Ekstig, B., Källne, E., Noreland, E., Manne, R.: *J. Phys. Chem. Solids* **30**, 1849 (1969)
19. Kurmaev, E. Z., Nemnonov, S. A., Menshikov, A. Z., Shveikin, G. P.: *Bull. Acad. Sci. USSR, Phys. Ser.* **31**, 1011 (1967)
20. Fischer, D. W., Baun, W. L.: *J. Appl. Phys.* **39**, 4757 (1968)
21. Holliday, J.: *J. Appl. Phys.* **38**, 4720 (1967)
22. Holliday, J.: *J. Phys. Chem. Solids* **32**, 1825 (1971)
23. Kurmaev, E. Z., Shveikin, G. P., Nemnonov, S. A.: *Phys. Stat. Sol. (b)* **60**, K65 (1973)
24. Brytov, I. A., Kurmaev, E. Z., Nemnonov, S. A.: *Fiz. metal metalloved* **26**, 366 (1968)

25. Brytov, I. A., Rumsh, M. A., Parabets, A. S.: *Sov. Phys. Solid State* **10**, 621 (1968)
26. Holliday, J., in: *Soft X-ray band spectra*, Fabian, D. J., Ed., p. 101. London-New York: Academic Press 1968
27. Ramqvist, L., Hamrin, K., Johanson, G., Fahlman, A., Nordling, C.: *J. Phys. Chem. Solids* **39**, 1835 (1969)
28. Ramqvist, L., Ekstig, B., Källne, E., Noreland, E., Manne, R.: *J. Phys. Chem. Solids* **32**, 149 (1971)
29. Ichikawa, K., Terasaki, O., Sagawa, T.: *J. Phys. Soc. Japan* **36**, 706 (1974)
30. Fischer, D. W.: *J. Appl. Phys.* **40**, 4151 (1969)
31. Menshikov, A. Z., Brytov, I. A., Kurmaev, E. Z.: *Phys. Stat. Sol.* **35**, 89 (1969)
32. Zhurakovskii, E. A., Vasilenko, N. N.: *Sov. Phys. Techn. Phys.* **14**, 710 (1970)
33. Brytov, I. A., Kurmaev, E. Z.: *Fiz. metal metalloved* **32**, 520 (1971)
34. Schwarz, K.: unpublished calculations
35. Weinberger, P., Schwarz, K., Neckel, A.: *J. Phys. Chem. Solids* **32**, 2063 (1971)
36. Trickey, S. B.: *Chem. Phys. Letters* **21**, 581 (1973)
37. Weinberger, P., Neckel, A.: *J. Phys. C. Solid State Phys.* **8**, 4001 (1975)

*Received February 2, 1976*